Chemical synthesis of perfectly isotactic and high melting bacterial poly(3-hydroxybutyrate) from bio-sourced racemic cyclic diolide

Xiaoyan Tang[1] & Eugene Y.-X. Chen [1]

Bacterial poly(3-hydroxybutyrate) (P3HB) is a perfectly isotactic, crystalline material possessing properties suitable for substituting petroleum plastics, but high costs and low volumes of its production are impractical for commodity applications. The chemical synthesis of P3HB via ring-opening polymerization (ROP) of racemic β-butyrolactone has attracted intensive efforts since the 1960s, but not yet produced P3HB with high isotacticity and molecular weight. Here, we report a route utilizing racemic cyclic diolide (rac-DL) derived from bio-sourced succinate. With stereoselective racemic catalysts, the ROP of rac-DL under ambient conditions produces rapidly P3HB with perfect isotacticity ([mm] > 99%), high melting temperature ($T_m = 171\,°C$), and high molecular weight ($M_n = 1.54 \times 10^5$ g mol^{-1}, $Đ = 1.01$). With enantiomeric catalysts, kinetic resolution polymerizations of rac-DL automatically stops at 50% conversion and yields enantiopure (R,R)-DL and (S,S)-DL with >99% e.e. and the corresponding poly[(S)-3HB] and poly[(R)-3HB] with high $T_m = 175\,°C$.

[1] Department of Chemistry, Colorado State University, Fort Collins, CO 80523-1872, USA. Correspondence and requests for materials should be addressed to E.-X.C. (email: eugene.chen@colostate.edu)

Poly(hydroxyalkanoate)s (PHAs)[1–12], naturally produced by bacteria and other living microorganisms from biorenewable resources such as carbohydrates and fats, are an important class of commercially implemented aliphatic polyesters as biodegradable and/or biocompatible materials for biomedical, pharmaceutical, and packaging applications[13–20]. The most prominent, thus most extensively studied, PHA is poly(3-hydroxybutyrate) (P3HB), in which bacterial poly[(R)-3-hydroxybutyrate], P[(R)-3HB], is a perfectly stereoregular, pure isotactic crystalline thermoplastic material[1–12]. Thanks to its comparable thermal and mechanical properties to those of high-performance isotactic polypropylene (it-PP), highly isotactic P3HB is being considered as an attractive biodegradable alternative to petroleum-based plastics, especially it-PP. However, high current production costs and limited production volumes of bacterial/microbial PHAs, including P3HB, render them impractical in many applications in areas such as biorenewable and biodegradable green commodity thermoplastics.

The chemical synthesis via ring-opening polymerization (ROP) of cyclic esters (lactones or lactides), a process typically catalyzed by a metal-based or organic catalyst, offers an alternative route to such technologically important biodegradable aliphatic polyesters[21–28], which is often advantageous, thanks to its fast kinetics of the polymerization, scalability of the polymer production, and tunability of catalysts and co-monomers. In this context, the ROP of β-butyrolactone (β-BL) has been developed for the chemical synthesis of P3HB[29–33], while the ROP of γ-butyrolactone (γ-BL) for the chemical synthesis of poly(4-hydroxybutyrate) (P4HB)[34, 35] has also been realized recently[36]. In the case of the ROP of β-BL, the cost-effective chemical synthesis of P3HB calls for the use of the racemic monomer, rac-β-BL, rather than the more expensive enantiopure (R)-β-BL, which requires a stereoselective ROP process to render the formation of isotactic P3HB. However, despite extensive research efforts since the 1960s, the chemical synthesis of P3HB with isotacticity P_m (defined as the probability of meso linkages between monomer units) >0.85 from the ROP of rac-β-BL has proven elusive. For example, the ROP of rac-β-BL by alkyl aluminoxanes produced a mixture of iso-enriched P3HB products as a whole ($P_m = 0.62$), which were fractionated into atactic and isotactic fractions with the highest P_m of 0.85 reported for the acetone-insoluble fraction[37–39]. A chiral initiator system consisting of ZnEt$_2$/(R)(−)-3,3-dimethyl-1,2-butanediol also yielded a mixture of P3HB products that were fractionated in methanol into soluble atactic and insoluble (~25%) isotactic (P_m ~ 0.80) fractions[40], and a chiral Co(salen)/Et$_3$Al complex afforded P3HB of low crystallinity (no tacticity data)[41]. A discrete β-

diiminate zinc alkoxide initiator promoted a controlled ROP of rac-β-BL with high polymerization rates, but the resulting P3HB is atactic[42]. Cr(III) salophen complexes converted rac-β-BL into iso-enriched P3HB with $P_m = 0.66$, medium number-average molecular weight ($M_n = 4.81 \times 10^4$ g mol^{-1}), high dispersity (Đ = 5.2), and modest melting-transition temperature ($T_m = 116$, 142 °C)[43]. Lanthanide (La, Nd) borohydrides supported on silica polymerized rac-β-BL into P3HB with $P_m = 0.85$ and $M_n = 1.15 \times 10^4$ g mol^{-1}[44]. It is worth noting that syndiotactic P3HB materials from being modestly syndiotactic (P_r ~ 0.70)[45, 46] to highly syndiotactic (P_r up to 0.95)[47–49], have been achieved through the ROP of rac-β-BL using alkyltinoxides and discrete yttrium complexes[50] supported by tetradentate, dianionic alkoxy-amino-bis(phenolate) [O^-,N,O,O^-] ligands, respectively. This Y catalyst system has also been utilized for the ROP of functional β-lactones, such as 4-allyloxymethylene-β-propiolactone, to afford either highly isotactic ($P_m = 0.93$, $M_n = 9.20 \times 10^3$ g mol^{-1}, Đ = 1.46) or syndiotactic ($P_r = 0.91$) polymer, depending on the substituents on the ligand[51]. In the context of creating a synthetic equivalent of bacterial P3HB, both high isotacticity ($P_m > 0.95$) and molecular weight ($M_n > 10^5$ g mol^{-1}) are typically required for practical use.

It is informative to point out that the ingenious utilization of a cyclic dimer of L-lactic acid (L-LA) rendered the commercial production of high-molecular-weight, highly isotactic polylactide (PLA)[52], but the efforts in attempting the chemical synthesis of high-molecular-weight, highly isotactic P3HB have so far been strictly limited to the use of the cyclic monomer of 3-hydroxybutyric acid (3HB), namely β-BL. β-Lactones are known to be carcinogenic (alkylating DNA)[53], and the competing ring-opening mechanisms (O-acyl vs. O-alkyl cleavage) were reported for the ROP of such highly strained monomers[54–56]. As the current approach via the ROP of rac-β-BL has yet so far produced P3HB with high molecular weight and high isotacticity (vide supra), we formulated the following three working hypotheses to address this long-standing challenge. First, by analogy of the PLA production, the chemical synthesis of P3HB could utilize a cyclic dimer of 3HB, namely eight-membered cyclic diolide (DL, Fig. 1), which is benign and can be readily derived from bio-sourced dimethyl succinate[57]. Worth noting here is that the enantiopure cyclic trimer of (R)-3HB, obtained in ~50% yield from the depolymerization of bacterial P[(R)-3HB][58], was attempted to polymerize back to P3HB but only low molecular weight (M_n ~ 5000 g mol^{-1}) oligomers were obtained[59, 60]. Second, as DL possesses two stereogenic centers, the ROP of its rac and meso diastereomers could lead to various stereoregular
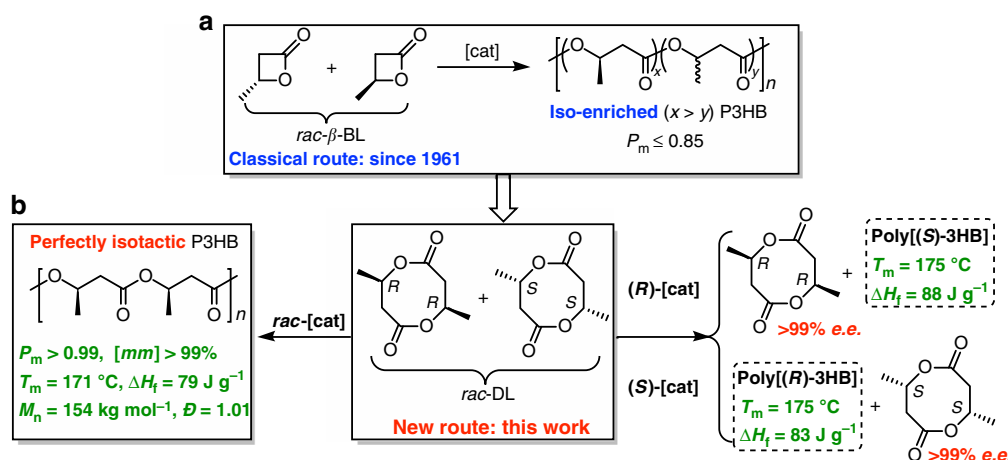

Fig. 1 Chemical synthesis routes to P3HB. **a** Classical route via the ROP of rac-β-BL to iso-enriched P3HB. **b** The new route via the ROP of rac-DL to perfectly isotactic P3HB. (P_m is the probability of meso linkages between HB units, and mm is isotactic triad made up of two adjacent meso diads)
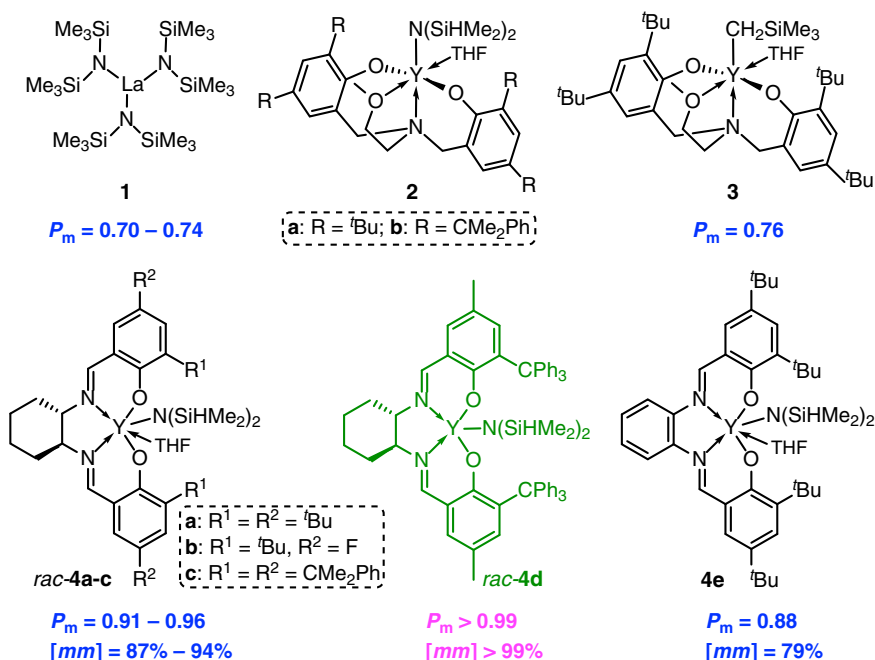
Fig. 2 Chemical structures of the catalysts. Structures of catalysts employed in this study for the ROP of *rac*-DL and the isotacticity of the resulting P3HB materials they produced. (P_m is the probability of meso linkages between HB units, and *mm* is isotactic triad made up of two adjacent *meso* diads)

Table 1 Results of *rac*-DL polymerization by yttrium catalysts 4a–e and BnOH initiator

Run	Catalyst	[*rac*-DL]/[4]	Time (min)	Conv.[a] (%)	M_n[b] (kg mol^{-1})	$Đ$[b] (M_w/M_n)	I^*[c] (%)	P_m[d]	[*mm*][d] (%)	T_m[e] (°C)
1	**4a**	20/1	20	100	4.77	1.17	74	0.91	87	128/136
2	**4a**	50/1	20	100	10.9	1.05	80	0.93	87	133/143
3	**4a**	100/1	20	100	23.0	1.04	75	0.94	89	136/145
4	**4a**	200/1	20	100	32.0	1.03	108	0.93	89	146
5	**4b**	100/1	20	100	25.1	1.03	69	0.95	89	147
6	**4b**	200/1	20	100	37.3	1.01	93	0.95	88	147
7	**4c**	100/1	20	100	25.7	1.11	67	0.96	93	153/157
8	**4c**	200/1	20	100	52.7	1.14	66	0.96	94	156
9	**4d**	100/1	20	100	20.1	1.07	86	0.99	98	161
10	**4d**	200/1	20	100	37.4	1.07	92	>0.99	>99	164
11	**4d**	400/1	20	100	64.3	1.02	107	>0.99	>99	169
12	**4d**	800/1	60	98	119	1.03	113	>0.99	>99	170
13	**4d**	1200/1	30	71	154	1.01	95	>0.99	>99	171
14	**4e**	100/1	20	100	23.7	1.03	73	0.88	79	121
15	**4e**	200/1	20	100	43.6	1.24	79	0.89	79	122

Conditions: *rac*-DL = 0.138 g (0.80 mmol), [*rac*-DL] = 1.0 M; DCM as the solvent, $V_{solvent}$ = 0.8 mL (except for run 13 where $V_{solvent}$ = 0.4 mL); room temperature; yttrium catalyst **4** to BnOH initiator ratio fixed at 1/1, and the amount varied according to the [*rac*-DL]/[**4**] ratio
[a]Conversions of monomers measured by ^{1}H NMR spectra of the quenched solution in benzoic acid/chloroform
[b]Weight-average molecular weights (M_w), number-average molecular weights (M_n), and dispersity indices ($Đ = M_w/M_n$) determined by GPC coupled with an 18-angle light scattering detector at 40 °C in chloroform
[c]The initiation efficiency $I^* = M_n$(calcd)/M_n(exptl), where M_n(calcd) = MW(*rac*-DL) × [*rac*-DL]/[**4**] × conv (%) + MW of chain-end groups (BnOH) = 172.18 × [*rac*-DL]/[**4**] × conv (%) + 108.14
[d]P_m is the probability of *meso* linkages between HB units, and *mm* is isotactic triad made up of two adjacent *meso* diads, determined by ^{13}C{^{1}H} NMR spectroscopy
[e]T_m measured by DSC with the cooling and second heating rate of 10 °C min^{-1} for samples produced by **4c–d**, 5 °C min^{-1} for samples produced by **4a–b**, or 2 °C min^{-1} for samples produced by **4e**

(isotactic, syndiotactic, stereoblock, etc.) P3HB materials, depending on the stereoselectivity of the catalyzed ROP process. Third, considering significantly increased sterics present in DL relative to β-BL, we should anticipate a higher degree of stereochemical control in the catalyzed ROP of DL, thereby potentially generating highly stereoregular P3HB materials.

Guided by the above three hypotheses, we have investigated this proposed DL route to P3HB and hereby disclose our discovery that the catalyzed ROP of *rac*-DL (Fig. 1) enables the highly efficient synthesis of P3HB with perfect isotacticity, high crystallinity, high melting temperature, and high molecular weight.

Results

Stereoselective ROP of *rac*-DL. Pure *rac*-DL can be synthesized in a multi-gram scale from bio-sourced dimethyl succinate (Supplementary Figs. 2–6; see Supplementary Information for details.). At the outset, the ROP of *rac*-DL was screened with La[N(SiMe$_3$)$_2$]$_3$ (**1**), a lanthanum complex that has been shown to be an effective catalyst for the ring-opening (co)polymerization of γ-BL and α-methylene-γ-butyrolactone (MBL)[36, 61, 62]. In combination with an alcohol initiator, the **1**/*x*BnOH (*x* = 2, 3, BnOH = benzyl alcohol) system was effective for the ROP of *rac*-DL (20 equiv) in dichloromethane (DCM) at room temperature (RT), achieving 100% conversion (*x* = 2) in 4 h or 98% (*x* = 3)
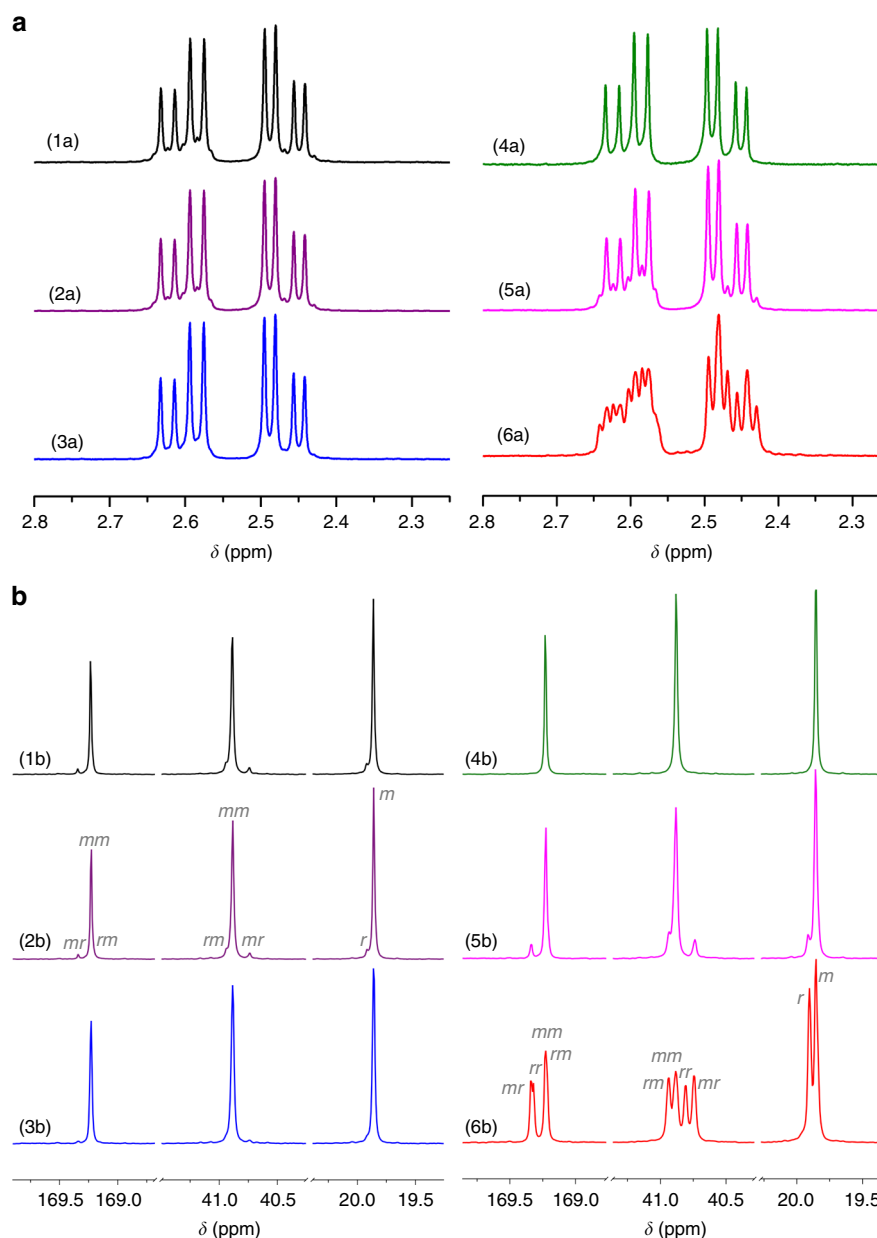
Fig. 3 Stereomicrostructures (tacticities) of P3HB. **a** ^{1}H NMR spectra (CDCl$_3$) in the methylene region. **b** ^{13}C NMR spectra (CDCl$_3$) in the carbonyl, methylene, and methyl regions. P3HB produced by (1a–b) [rac-DL]/[**4a**] = 200/1; (2a–b) [rac-DL]/[**4b**] = 200/1; (3a–b) [rac-DL]/[**4c**] = 200/1; (4a–b) [rac-DL]/[**4d**] = 200/1; (5a–b) [rac-DL]/[**4e**] = 200/1; and (6a–b) comparative example of [rac-β-BL]/[**4d**] = 100/1

conversion in 8 h, but the resulting P3HB exhibited a low molecular weight ($M_n = 2.43 \times 10^3$ g mol^{-1} and $Đ = 1.09$ for $x = 3$, Supplementary Table 1). Furthermore, both ^{1}H and ^{13}C NMR spectra (Supplementary Figs. 32, 33) showed the formation of an iso-biased amorphous material ($P_m = 0.74$, $x = 2$; $P_m = 0.70$, $x = 3$), which was confirmed by observation of only glass-transition temperature (T_g) on its differential scanning calorimetry (DSC) curves (Supplementary Fig. 34). Next, we turned to a "privileged class of catalysts" for the ROP of cyclic esters[21], discrete yttrium amido complexes **2** (**a**, R = ^{t}Bu; **b**, R = CMe$_2$Ph) and alkyl complex **3** supported by the tetradentate [O$^-$,N,O,O$^-$] ligand (Fig. 2), which were previously shown to be superior catalysts for the ROP of γ-BL and MBL[36, 61, 62] as well as highly active catalysts for the syndiospecific ROP of rac-β-BL[47–49]. With a high precatalyst loading of 5 mol% and in combination with 1 equiv of BnOH initiator that undergoes instantaneous alcoholysis of the yttrium complex to generate the corresponding yttrium alkoxide

catalyst[47–50], all three yttrium complexes were active for the ROP of rac-DL, with yttrium alkyl **3** being the most active but still rather sluggish (76% conversion after 32 h). Moreover, these catalysts incorporating the tripodal alkoxy-amino-bis(phenolate) ligand afforded only low-molecular-weight ($M_n = 2.70 \times 10^3$ g mol^{-1} and $Đ = 1.08$ for catalyst **3**), iso-biased amorphous material ($P_m = 0.76$, Supplementary Table 1, Supplementary Figs. 35, 36). For catalysts **2**, only low conversions were achieved even after 48 h (44% by **2a**; 17% by **2b**), and the P3HB products were not isolated but the estimated P_m values by in situ NMR spectra were similar to that by catalyst **3**.

Considering the steric hindrance of rac-DL monomer with the eight-membered-ring framework and the low activity and isoselectivity of also sterically encumbered catalysts **1–3** screened, we arrived at sterically more open yttrium racemic salen complexes **4a–e** (Fig. 2). Yttrium silylamido complexes **4a–d** supported by N,N′-bis(salicylidene)cyclohexanediimine (salcy)

ligands and complex **4e** supported by the analogous salph ligand were readily synthesized in good yields (58–83%, see Supplementary Information for details, Supplementary Figs. 13–22) according to the procedures established for the synthesis of known complex **4a**[63, 64] and known salen ligands (Supplementary Figs. 7–13)[65–71]. Complex **4a** with the classic salen ligand bearing the 3, 5-di-*tert*-butyl substituents was first examined for its activity and stereoselectivity towards the ROP of *rac*-DL. Excitingly, this complex, when combined with 1 equiv of BnOH initiator, rapidly polymerized 20–200 equiv of *rac*-DL to completion within 20 min at RT. The molecular weight of the resulting P3HB increased from low $M_n = 4.77 \times 10^3$ g mol^{-1} ($Đ$ = 1.17) to medium $M_n = 3.20 \times 10^4$ g mol^{-1} ($Đ$ = 1.03) with increasing the [*rac*-DL]/[**4a**] ratio from 20/1 to 200/1, and the calculated initiation efficiency ranged from 74 to 108% (runs 1–4, Table 1), all indicating a controlled polymerization. More importantly, complex **4a** now yielded isotactic P3HB with P_m ~ 0.91–0.94 and isotactic [*mm*] triad ~ 87–89% based on ^{1}H and ^{13}C NMR analysis (Fig. 3). Accordingly, the resulting P3HB material became crystalline, exhibiting a T_m ~ 136–146 °C, depending on the polymer molecular weight (runs 1–4, Table 1). Replacing the initiator BnOH with ^{i}PrOH lowered the polymerization activity by threefold, now requiring 60 min to achieve complete monomer (200 equiv) conversion. Furthermore, the molecular weight ($M_n = 6.07 \times 10^4$ g mol^{-1}) of the resulting P3HB was considerably higher than the theoretical value, thus giving rise to a low initiation efficiency of only 57%, although the P3HB tacticity remained the same. Other alcohols such as Ph$_2$CHCH$_2$OH were also found less effective than BnOH. Therefore, all the subsequent polymerization studies with other yttrium complexes (**4b**–**e**) employed exclusively BnOH as the more effective initiator.

The above exciting results brought about by yttrium salen complex **4a** prompted us to investigate possible effects of the salen ligand framework's electronics, sterics, and geometry of the backbone diimine linker on the *rac*-DL polymerization activity and stereoselectivity. In the context of electronic effects, electron withdrawing substituents (e.g., F) introduced to the 5-positions of the salicylidene framework were found to generate a more redox stable and active (salcy)Co(III) catalyst for the copolymerization of epoxide and anhydride monomer pairs[65]. In the present polymerization of *rac*-DL by (salcy)yttrium catalyst **4b** with the F groups substituted at the 5-positions of the salcy ligand, only the isotacticity of the resulting P3HB was improved slightly to now $P_m = 0.95$ and $T_m = 147$ °C (runs 5 and 6, Table 1), as compared with the parent *tert*-butyl substituted catalyst **4a**. Turning to the steric perturbation of the catalyst, the more bulky cumyl-substituted complex **4c** produced isotactic P3HB with a noticeably higher isotactic [*mm*] triad of 94% (Fig. 3) and T_m of 156 °C (run 8, Table 1), relative to the [*mm*] of 89% and T_m of 146 °C for the P3HB produced by catalyst **4a** under identical conditions (run 4 vs. 8, Table 1). These results showed much more pronounced effects of the ligand sterics than electronics on the polymerization stereoselectivity. Hence, the even more bulky trityl (Ph$_3$C) groups were substituted at the 3-positions of the salcy ligand framework to generate catalyst racemic **4d**. Remarkably, catalyst **4d** produced essentially stereo-perfect, pure isotactic P3HB with $P_m > 0.99$ and [*mm*] > 99% (run 10, Table 1), while maintaining high polymerization activity (100% monomer conversion in 20 min). Consistent with this NMR-derived stereo-microstructure (Fig. 3), the resulting crystalline isotactic P3HB exhibited a high T_m of 164 °C. Lastly, to probe the possible effects of the geometry of the backbone diimine linker, we examined the performance of the salph-based complex **4e** for the *rac*-DL polymerization and found that this catalyst afforded P3HB with a considerably lower isotacticity (P_m ~ 0.88–0.89, [*mm*] = 79%,
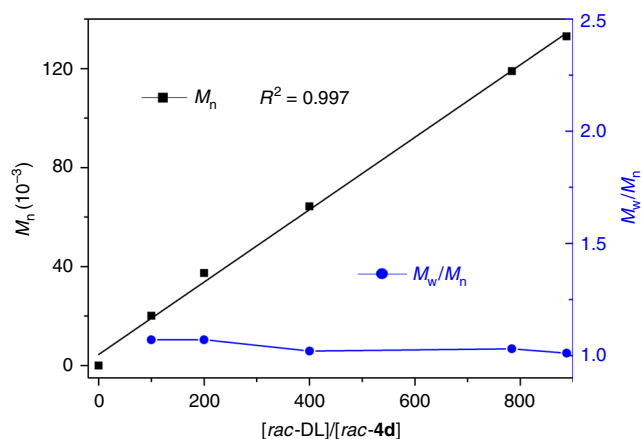
Fig. 4 Degree of control over the molecular weight and dispersity in the ROP of *rac*-DL. Plots of M_n and $Đ$ values of isotactic P3HB produced by racemic catalyst **4d** at varied [*rac*-DL]/[*rac*-**4d**] ratios. The runs at 800/1 and 1200/1 ratios under the same conditions (0.8 mL DCM, 60 min) did not achieve quantitative conversions; thus, the ratios used for the plot were adjusted by their conversions (98% and 74%, respectively)

runs 14 and 15), as compared with the salcy-based analogue complex **4a** under identical conditions (P_m ~ 0.93–0.94, [*mm*] = 89%, runs 3 and 4). It is worth noting here that the high stereoselectivity of catalysts **4** observed for the ROP of *rac*-DL does not apply to the ROP of *rac*-β-BL; for example, the ROP of *rac*-β-BL by the best catalyst of the series, **4d**, was not only sluggish (even with a high catalyst loading of 1.0 mol% the reaction required 8 h to achieve 96% monomer conversion) but also non-stereoselective, producing atactic P3HB (Fig. 3, Supplementary Fig. 40). These results further highlight the importance of the steric interplay and matching between the catalyst and monomer structures to achieve a highly stereoselective ROP of such racemic lactone and diolide monomers.

Having identified catalyst **4d** being the best catalyst of this series, we further examined the ability of this catalyst to control the molecular weight so that practically useful high-molecular-weight isotactic P3HB with $M_n > 10^5$ g mol^{-1} could be synthesized. To this end, we varied the [*rac*-DL]/[**4d**] feed ratio from 100/1 to 1200/1 and found that the molecular weight of the resulting P3HB increased linearly ($R^2 = 0.997$, Fig. 4) from medium $M_n = 2.01 \times 10^4$ g mol^{-1} ($Đ = 1.07$) to high $M_n = 1.54 \times 10^5$ g mol^{-1} ($Đ = 1.01$), while all the $Đ$ values remained low in a narrow range from 1.01 to 1.07 (runs 9–13, Table 1). These observations, coupled with the calculated high initiation efficiencies of >86% for all the polymerization runs by catalyst **4d**, pointed to a well-controlled ROP of *rac*-DL.

Thermal properties. DSC curves of the isotactic P3HB materials produced by the ROP of *rac*-DL with catalysts **4a**–**4d** under identical conditions ([*rac*-DL]/[**4**] = 200/1, DCM, RT, 20 min, 100% conversion) are compared in Fig. 5. Consistent with the gradual increase of the isotacticity of P3HB on going from **4a** to **4d**, the T_m value was observed to increase from 146 (**4a**) to 147 (**4b**), 156 (**4c**), and 164 °C (**4d**). Noteworthy also is the steadily enhanced heat of fusion (ΔH_f) from **4a** to **4d**: 40.9, 47.0, 56.5, and 79.3 J g^{-1}, which corresponds to an increase in the P3HB crystallinity from 28 to 32, 39, and 54%, relative to the estimated ΔH_f^0 value (146 J g^{-1}) for an infinite crystal of 100% crystalline P3HB (Supplementary Note 1)[72]. Furthermore, the T_m value of the perfectly isotactic P3HB produced by catalyst **4d** depends somewhat on the polymer M_n: when M_n was enhanced from 2.01×10^4 to 3.74×10^4, 6.43×10^4, 1.19×10^5, and 1.54×10^5 g
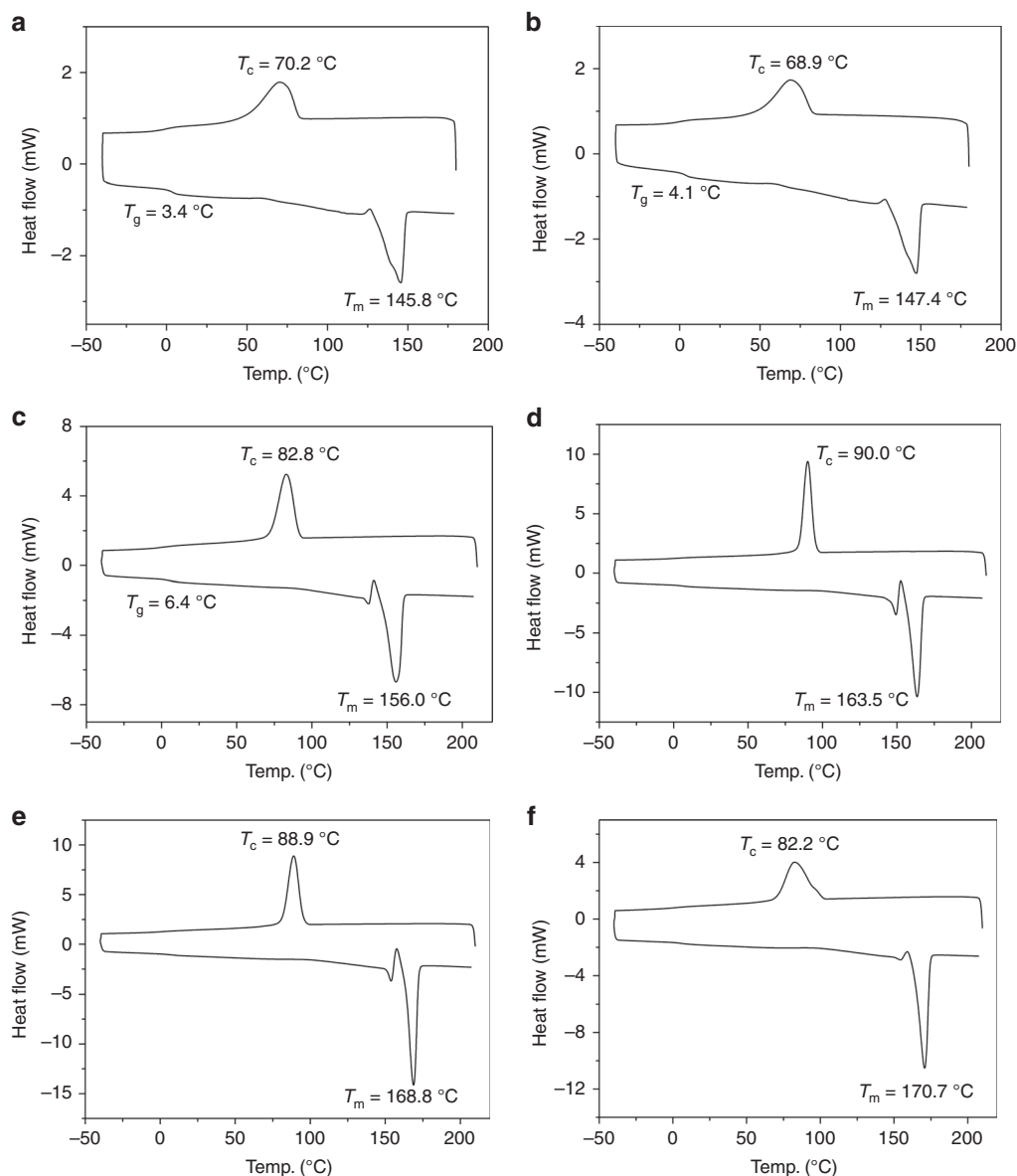
Fig. 5 Thermal properties of P3HB derived from the ROP of *rac*-DL. **a** [*rac*-DL]/[**4a**] = 200/1 (ΔH_f = 40.9 J g^{-1}). **b** [*rac*-DL]/[**4b**] = 200/1 (ΔH_f = 47.0 J g^{-1}). **c** [*rac*-DL]/[**4c**] = 200/1 (ΔH_f = 56.5 J g^{-1}). **d** [*rac*-DL]/[**4d**] = 200/1 (ΔH_f = 79.3 J g^{-1}). **e** [*rac*-DL]/[**4d**] = 400/1 (ΔH_f = 80.4 J g^{-1}). **f** [*rac*-DL]/[**4d**] = 1200/1 (ΔH_f = 78.6 J g^{-1}). Crystallization temperature (T_c) and melting-transition temperature (T_m) taken from the cooling and second heating scans, respectively
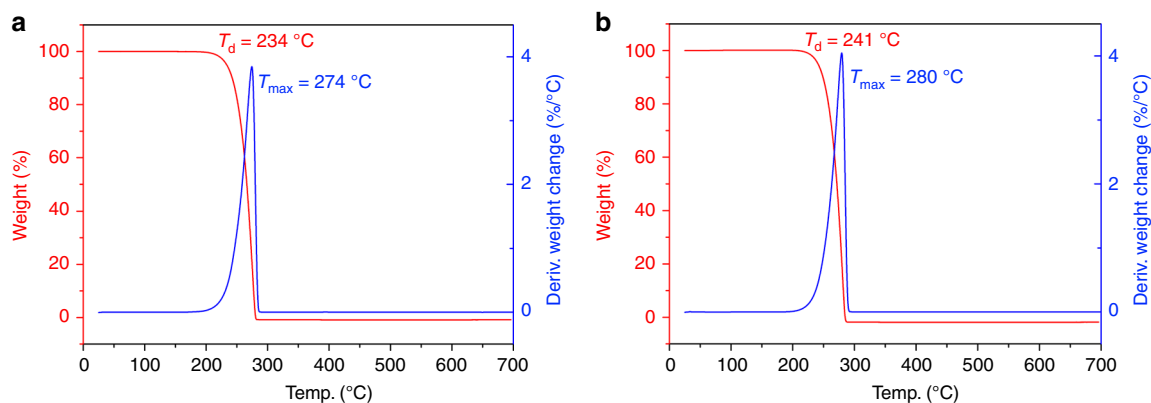

Fig. 6 Thermal stability of P3HB derived from the ROP of *rac*-DL. **a** TGA and DTG of P3HB produced by catalyst **4a**, M_n = 3.20 × 10^4 g mol^{-1}, Đ = 1.03, [*mm*] = 89%. **b** TGA and DTG of P3HB produced by catalyst **4d**, M_n = 1.19 × 10^5 g mol^{-1}, Đ = 1.03, [*mm*] > 99%

Table 2 Results of *rac*-DL polymerization by yttrium catalysts (*R,R*)- and (*S,S*)-4d/BnOH

Run	Catalyst	[*rac*-DL]/[4d]	Time (min)	Conv. (%)	M_n (kg mol^{-1})	Đ (M_w/M_n)	[*mm*] (%)	$T_m{}^a$ (°C)	$[\alpha]_D{}^{23}$ (°)[b]	e.e.[c] (%)
1	(*R,R*)-**4d**	400/1	20	~50	43.0	1.07	>99	172	−94.8	>99
2	(*R,R*)-**4d**	800/1	20	~50	74.8	1.05	>99	172	−94.5	>99
3	(*R,R*)-**4d**	1600/1	60	43	118	1.09	>99	175	−73.6	80
4	(*S,S*)-**4d**	400/1	20	~50	42.9	1.08	>99	172	+93.7	>99
5	(*S,S*)-**4d**	800/1	20	~50	72.1	1.04	>99	172	+94.6	>99
6	(*S,S*)-**4d**	1600/1	60	44	113	1.07	>99	175	+76.1	85

Conditions: *rac*-DL = 0.241 g (1.40 mmol), [*rac*-DL] = 1.0 M in DCM (1.4 mL); room temperature. See footnotes in Table 1 for other explanations
$^a T_m$ measured by DSC with the cooling and second heating rate of 10 °C min^{-1}
^{b}Specific rotation ($[\alpha]_D{}^{23}$) of the unreacted monomer (DL) in chloroform
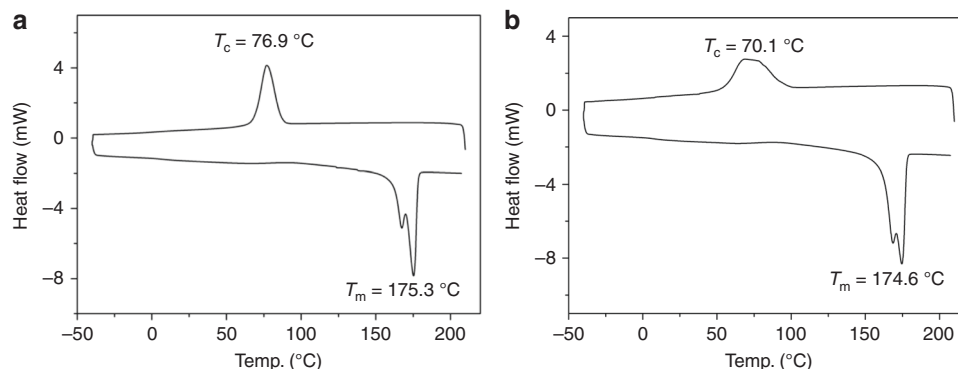^{c}Enantiomeric excess (e.e.) determined by chiral HPLC

Fig. 7 DSC curves of poly[(*R*)-3HB] materials. **a** Produced via chemical ROP of *rac*-DL by (*S,S*)-[**4d**]. **b** Commercial natural poly[(*R*)-3-hydroxybutyric acid] purchased from Sigma-Aldrich. T_c and T_m values taken from the cooling and second heating scans, respectively

mol^{-1} (runs 9–13, Table 1), T_m increased accordingly from 161 to 164, 169, 170, and 171 °C. These are perfectly isotactic, highly crystalline materials, with high ΔH_f values of ~ 80 J g^{-1} (Fig. 5, Supplementary Fig. 40).

Thermal degradation profiles of the selected isotactic P3HB samples derived from the ROP of *rac*-DL by racemic catalysts **4a** and **4d** were examined by thermal gravimetric analysis (TGA). As can be seen from the TGA and derivative thermogravimetry (DTG) curves (Fig. 6), the P3HB produced by **4a** ($M_n = 3.20 \times 10^4$ g mol^{-1}, Đ = 1.03, [*mm*] = 89%) exhibited a decomposition temperature (T_d) (defined by the temperature of 5% weight loss in the TGA curve) of 234 °C and a maximum rate decomposition temperature (T_{max}) of 274 °C, which put the $T_d \sim 90$ °C above its T_m, proving a window for melt processing. A P3HB sample produced by **4d** with a similar M_n (3.74 × 10^4 g mol^{-1}) but a much higher isotacticity of [*mm*] > 99% exhibited a somewhat higher T_d of 239 °C and T_{max} of 281 °C (Supplementary Fig. 41). Keeping the tacticity the same ([*mm*] > 99%) while increasing the molecular weight to $M_n = 1.19 \times 10^5$ g mol^{-1} enhanced the T_d only slightly to 241 °C (Fig. 6).

Kinetic resolution and mechanistic considerations. The above results demonstrated that the polymerization of *rac*-DL by *rac*-**4d** produced P3HB with essentially perfect isotacticity. However, these exciting results also brought about three important fundamental questions: (1) Can enantiomeric catalysts (*R,R*)-**4d** and (*S,S*)-**4d** kinetically resolve racemic monomer *rac*-DL? (2) What is the stereocontrol mechanism—enantiomorphic-site control or chain-end control? (3) What is the isotactic polymer stereomicrostructure—1:1 mixture of poly[(*R,R*)-DL] and poly[(*S,S*)-DL], stereoblock of poly(*rac*-DL), or tapered block copolymer poly[(*R,R*)-DL]-*co*-[(*S,S*)-DL]?

To address these questions, the corresponding enantiomeric catalysts (*R,R*)-**4d** and (*S,S*)-**4d** have been successfully synthesized and subsequently employed to perform kinetic resolution polymerization of *rac*-DL with both enantiomeric catalysts (See Supplementary Information for details, Supplementary Figs. 23–29), the results of which are summarized in Table 2. In sharp contrast to the polymerization by *rac*-**4d** with a [*rac*-DL]/[*rac*-**4d**] ratio of 400 or 800 that achieved a quantitative monomer conversion after 20 min, the same polymerization by (*R,R*)-**4d** or (*S,S*)-**4d** achieved a conversion of ~50% (runs 1–2 and 4–5, Table 2), after which no further monomer conversion can be achieved, even after extended times (6 h), indicative of exclusive catalyst site selectivity for the ROP of one particular enantiomer of the monomer. Characterizations of the ~50% unreacted, pure monomer showed to exhibit identical NMR spectra to that of *rac*-DL (Supplementary Fig. 42); the specific rotation of the unreacted monomer produced by (*R,R*)-**4d** was measured to be from −94.8° to −94.5° (runs 1–2, Table 2), which agrees well with the reported value of (*R,R*)-DL[57], while the specific rotation of the unreacted monomer by (*S,S*)-**4d** was from +93.7 to +94.6 (runs 4–5, Table 2), which is assigned to be (*S,S*)-DL accordingly. The enantiomeric excess (e.e.) of the unreacted monomer was determined by chiral HPLC coupled with a Chiralcel OD-H column to be >99% e.e. (Supplementary Figs. 55, 56 and 58, 59) for all the runs with conversion at ~50% (runs 1–2 and 4–5, Table 2). It is noted here that the [*rac*-DL]/[**4d**] = 1600 runs achieved 43–44% conversion after 60 min (runs 3 and 6); accordingly, the e.e.'s of the unreacted monomer was only 80–85%, respectively (Supplementary Figs. 57 and 60). Overall, these results indicate that (*R,R*)-**4d** exhibits exclusive selectivity for the ROP of (*S,S*)-DL, while (*S,S*)-**4d** polymerizes (*R,R*)-DL exclusively. Based on the quantitative e.e.'s (>99%) for the optically resolved, unreacted monomer, the stereoselectivity factor *s* for both enantiomeric catalysts was calculated to be >10^3.
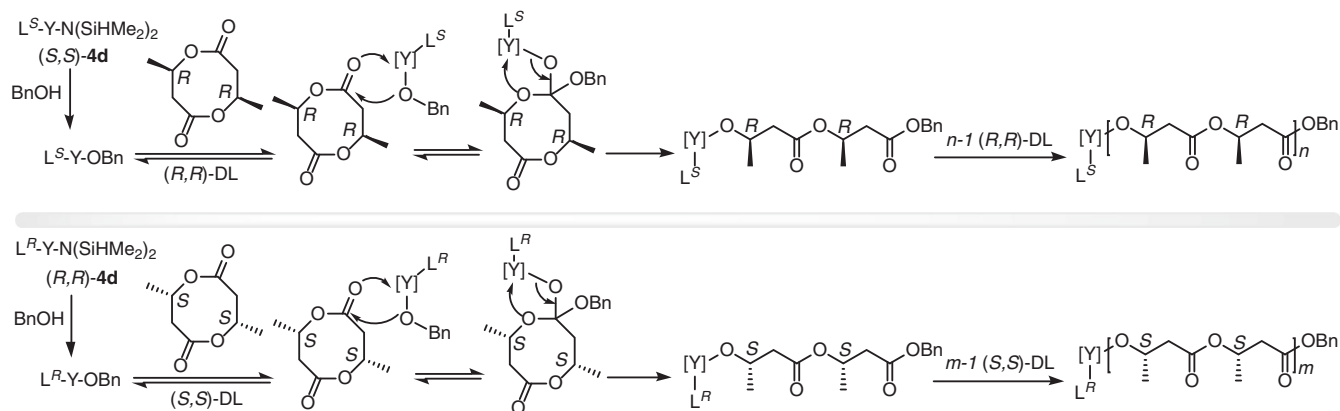
Fig. 8 Proposed mechanism. Chemical scheme of the proposed catalyst-site controlled coordination-insertion mechanism for the ROP of *rac*-DL by *rac*-**4d**

These profound results also indicated an enantiomorphic-site control mechanism for the stereoselective ROP process.

This essentially perfect stereoselectivity enabled the synthesis of enantiomeric poly[(R,R)-DL] and poly[(S,S)-DL] using (S,S)-**4d** and (R,R)-**4d**, respectively. The T_m values (Table 2, Supplementary Fig. 43) of these enantiopure polymers are somewhat higher (by 3–5 °C) than those of isotactic poly(*rac*-DL) with similar molecular weights, prepared by *rac*-**4d**, and also higher (by 5–7 °C) than that of 1:1 mixture of poly[(R,R)-DL] and poly[(S,S)-DL] (Supplementary Figs. 44–46), indicating no stereocomplexation between two enantiomeric P3HB chains. These enantiopure polymers also exhibit high ΔH_f values in the range of 79–88 J g^{-1}, comparable to that of natural poly[(R)-3HB]. The highest T_m of 175 °C was achieved by the enantiomeric polymers with $M_n =$ 113–118 kg mol^{-1} (runs 3 and 6, Table 2), which, along with the heat of fusion value, is essentially identical to that of the commercial natural poly[(R)-3HB] (Fig. 7).

To gain further insight into the stereomicrostructure of the highly isotactic P3HB produced by *rac*-**4d**, the polymers produced at different times and [*rac*-DL]/[*rac*-**4d**] ratios were analyzed by matrix-assisted laser desorption/ionization time-of-flight mass spectroscopy (MALDI-TOF MS). When a low ratio of 20/1 was used with a longer reaction time (20 min), the mass spectra showed the pronounced transesterification side reaction, as evidenced by the appearances of molecular ion peaks with the spacing between the neighboring peaks being that of the half molar mass of the repeat unit, DL ($m/z = 172.07$) (Supplementary Fig. 47), which also resulted in a higher dispersity ($Đ = 1.20$) and lower isotacticity ($P_m = 0.96$). Under these conditions, the microstructure of the resultant isotactic P3HB is a stereoblock polymer, poly[(R)-3HB]-*b*-poly[(S)-3HB], as a result of transesterification after the reaction reached full conversion (Supplementary Fig. 50). Consistent with this reasoning, when the polymerization was quenched after 30 s (at which time the full conversion was also achieved), the dispersity of the resulting polymer decreased to $Đ = 1.09$, and its mass spectrum displayed nearly exclusive molecular ion peaks with the spacing between the neighboring peaks being that of *rac*-DL, with just minor peaks with extremely low intensity for the odd 3-HB units (Supplementary Fig. 51). These results indicate that the transesterification side reaction occurred when the reaction reached full conversion and thus can be essentially shut down by reducing the polymerization time. In this case, the resulting polymer is predominantly a mixture of poly[(R)-3HB] and poly[(S)-3HB], with only a trace amount of stereoblock polymer, poly[(R)-3HB]-*b*-poly[(S)-3HB]. Obviously, the transesterification side reaction can also be shut down by reducing the catalyst amount in feed with the same reaction time, giving the polymers with very low dispersity indices ($Đ = 1.01–1.03$) at higher [*rac*-DL]/[*rac*-**4d**] feeding ratios. Furthermore, this transesterification side reaction can be shut down by the use of enantiomeric pure catalysts (Supplementary Figs. 52, 53). Overall, the polymerization of *rac*-DL by *rac*-**4d**, when stopped at full conversion (i.e., no transesterification side reactions), produces a mixture of poly[(R)-3HB] and poly[(S)-3HB] (Fig. 8), due to its exclusive (R,R)-**4d**/(S,S)-DL and (S,S)-**4d**/(R,R)-DL catalyst/monomer selectivity as demonstrated by the kinetic resolution results.

Discussion

The approach via the ROP of the bio-sourced *rac*-DL has successfully addressed the 50+-year challenge in the chemical synthesis of bacterial P3HB. This success was enabled by the specifically designed stereoselective molecular catalyst and its steric interplay with the monomer structure, thereby producing the desired P3HB material with perfect isotacticity ([mm] > 99%), high crystallinity, and melting temperature ($T_m = 171$ °C), as well as high molecular weight and low dispersity ($M_n = 154$ kg mol^{-1}, $Đ = 1.01$). This novel ROP of *rac*-DL also exhibits a high polymerization rate and efficiency. The resulting highly isotactic P3HB by *rac*-**4d** is shown to be the mixture of poly[(R)-3HB] and poly[(S)-3HB] when the polymerization is stopped at full conversion. Thanks to the exclusive (R,R)-**4d**/(S,S)-DL and (S,S)-**4d**/(R,R)-DL catalyst/monomer selectivity, kinetic resolution polymerization of *rac*-DL with enantiomeric catalysts automatically ceases at 50% conversion and yields enantiopure (R,R)-DL and (S,S)-DL with >99% *e.e.* and the corresponding poly[(S)-3HB] and poly[(R)-3HB] with high $T_m = 175$ °C and crystallinity, which is essentially identical to that of the commercial natural poly[(R)-3HB].

The tunability of the catalyst structure allows a rapid entry to P3HB materials with various tacticities (thus tunable thermal and mechanical properties) and predicted molecular weights with low dispersity indices (vs. a typical $Đ$ value of ~2.0 for bacterial P3HB). In addition, the molecular catalysts should allow copolymerization of *rac*-DL with other monomers to produce 3HB-based copolymers. Altogether, this ROP of DL represents a paradigm shift in the chemical synthesis of P3HB and opens up a plethora of opportunities for discovering new catalysts, materials, and processes in the ROP of *rac*-DL and other diastereomers of 3HB cyclic dimers or trimers, and so on.

Methods

Materials and instruments. All syntheses and manipulations of air- and moisture-sensitive chemicals and materials were carried out in flamed Schlenk-type glassware on a dual-manifold Schlenk line or in an inert gas (Ar or N$_2$)-filled glovebox. NMR-scale reactions were conducted in Teflon-valve-sealed J. Young-type NMR tubes. HPLC-grade organic solvents were first sparged extensively with

nitrogen during filling 20 L solvent reservoirs and then dried by passage through activated alumina (for DCM) followed by passage through Q-5 supported copper catalyst (for toluene and hexanes) stainless steel columns. Benzene-d_6 was dried over sodium/potassium alloy and filtered, whereas CD_2Cl_2 and $CDCl_3$ were dried over CaH_2, vacuum-distilled and stored over activated Davison 4 Å molecular sieves. HPLC chromatograms were obtained on an Agilent 1100 series system using a Chiralcel OD-H column with hexanes/isopropanol (80/20) as the eluent at a flow rate of 1.0 mL min^{-1}. Optical rotations were measured with an Autopol-III automatic polarimeter. NMR spectra were recorded on a Varian Inova or Bruker AV-III 400 MHz spectrometer (400 MHz, ^{1}H; 100 MHz, ^{13}C). Chemical shifts for ^{1}H and ^{13}C spectra were referenced to internal solvent resonances and are reported as parts per million relative to SiMe$_4$. Elemental analyses were performed by Robertson Microlit Laboratories, Madison, NJ.

Tri[N,N-bis(trimethylsilyl)amide] lanthanum(III) La[N(SiMe$_3$)$_2$]$_3$ (1), yttrium chloride YCl$_3$, and (trimethylsilyl)methyllithium (SiMe$_3$)$_2$CH$_2$Li solution in pentane were purchased from Sigma-Aldrich Chemical Co. and used as received. 2,2-Diphenylethanol was purchased from Aldrich Chemical Co., which were purified by sublimation twice. Isopropanol and benzyl alcohol were purchased from Fisher Scientific Co. and Alfa Aesar Chemical Co., respectively, which were purified by distillation over CaH$_2$ and stored over activated Davison 4 Å molecular sieves. Dimethyl succinate, sodium methoxide, and 3-chloroperoxybenzoic acid (mCPBA, 70–75%) were purchased from Fisher Scientific Co. and used as received. Iodomethane was purchased from Alfa Aesar Chemical Co. and used as received.

General polymerization procedures. Polymerizations were performed in 5.5 mL glass reactors inside the inert glovebox at RT. The reactor was charged with a predetermined amount of catalyst and/or initiator and solvent (as specified in the polymerization tables) in a glovebox. The mixture was stirred at RT for 10 min, and the polymerization was initiated by rapid addition of rac-DL solution. After a desired time period, the polymerization was immediately quenched by addition of 0.5 mL of benzoic acid/chloroform (10 mg mL^{-1}) and a 0.02 mL of aliquot was taken from the reaction mixture and prepared for ^{1}H NMR analysis to obtain the percent monomer conversion data. The quenched mixture was then precipitated into 50 mL of cold methanol while stirring, filtered, washed with cold methanol to remove any unreacted monomer, and dried in a vacuum oven at RT overnight to a constant weight.

Procedures for kinetic resolution of rac-DL by enantiomeric Y complexes (R,R)-4d and (S,S)-4d. rac-DL was polymerized by (R,R)-4d or (S,S)-4d according to the above general procedure. The conversion of monomer was ~50% with the [rac-DL]/[(R,R)-4d] molar ratio of 400 or 800 after 20 min, under which the conversion was 100% with rac-4d as the catalyst. The polymerization was then quenched with benzoic acid/DCM (caution: avoid using nucleophiles such as methanol or acidified methanol as they react with the unreacted monomer, see Supplementary Figs. 30, 31). The solvent was evaporated, and the solid residue was sublimated at 40–50 °C under vacuum to recover the pure unreacted monomer. The residue in the sublimator was dissolved in about 2 mL DCM, precipitated into 60 mL MeOH, filtrated, washed, and dried in vacuum to recover the polymer. The recovered unreacted monomer was analyzed by a chiral HPLC system to measure e.e. values, and the stereoselectivity factor s was calculated from Eq. (1):

$$S = \frac{\ln[(1-c)(1-ee_m)]}{\ln[(1-c)(1+ee_m)]} \qquad (1)$$

where $c = 1 - \frac{[S]+[R]}{[S]_0+[R]_0}$, $ee_m = \frac{[S]-[R]}{[S]+[R]}$.

Polymer characterizations. Measurements of polymer absolute weight-average molecular weight (M_w), number-average molecular weight (M_n), and molecular weight distributions or dispersity indices ($Đ = M_w/M_n$) were performed via gel-permeation chromatography (GPC). The GPC instrument consisted of an Agilent HPLC system equipped with one guard column and two PLgel 5 μm mixed-C gel permeation columns and coupled with a Wyatt DAWN HELEOS II multi (18)-angle light scattering detector and a Wyatt Optilab TrEX dRI detector; the analysis was performed at 40 °C using chloroform as the eluent at a flow rate of 1.0 mL min^{-1}, using Wyatt ASTRA 7.1.2 molecular weight characterization software (some presentative GPC traces are shown in Supplementary Figs. 61–66). The refractive index increment (dn/dc) of P3HB was determined to be 0.0254 ± 0.0004 mL g^{-1}, obtained by batch experiments using Wyatt Optilab TrEX dRI detector and calculated using ASTRA software. Polymer solutions were prepared in chloroform and injected into dRI detector by Harvard Apparatus pump 11 at a flow rate of 0.25 mL min^{-1}. A series of known concentrations were injected and the change in refractive index was measured to obtain a plot of change in refractive index vs. change in concentration ranging from 0.4 to 4.0 mg mL^{-1}. The slope from a linear fitting of the data was the dn/dc of the polymer.

The isolated low molecular weight samples were analyzed by MALDI-TOF MS; the experiment was performed on Microflex-LRF mass spectrometer (Bruker Daltonics, Billerica, MA) operated in positive ion, reflector mode using a Nd:YAG laser at 355 nm and 25 kV accelerating voltage. A thin layer of a 1% NaI solution was first deposited on the target plate, followed by 0.6 μL of both sample and matrix (dithranol in chloroform) in chloroform. External calibration was done using a peptide

calibration mixture (4–6 peptides) on a spot adjacent to the sample. The raw data was processed in the FlexAnalysis software (version 3.4.7, Bruker Daltonics).

T_m and T_g were measured by DSC on an Auto Q20, TA Instrument. All T_m and T_g values were obtained from a second scan after the thermal history was removed from the first scan. The second heating rate was 10 °C min^{-1} and cooling rate was 10 °C min^{-1} unless indicated otherwise in the polymerization tables. T_d, defined by the temperature of 5% weight loss, and T_{max} of the polymers were measured by TGA on a Q50 TGA Analyzer, TA Instrument. Polymer samples were heated from ambient temperatures to 700 °C at a heating rate of 10 °C min^{-1}. Values of T_{max} were obtained from derivative (wt%/°C) vs. temperature (°C) plots, while T_d and T_{onset} values (initial and end temperatures) were obtained from wt% vs. temperature (°C) plots.

References

1. Anjum, A. et al. Microbial production of polyhydroxyalkanoates (PHAs) and its copolymers: a review of recent advancements. *Int. J. Biol. Macromol.* **89**, 161–174 (2016).
2. Muhammadi, S., Afzal, M. & Hameed, S. Bacterial polyhydroxyalkanoates-eco-friendly next generation plastic: production, biocompatibility, biodegradation, physical properties and applications. *Green Chem. Lett. Rev.* **8**, 56–77 (2015).
3. Laycock, B., Halley, P., Pratt, S., Werker, A. & Lanta, P. The chemomechanical properties of microbial polyhydroxyalkanoates. *Prog. Polym. Sci.* **38**, 536–583 (2013).
4. Somleva, M. N., Peoples, O. P. & Snell, K. D. PHA bioplastics, biochemicals, and energy from crops. *Plant Biotechnol. J.* **11**, 233–252 (2013).
5. Taguchi, S., Iwata, T., Abe, H. & Doi, Y. in *Polymer Science: A Comprehensive Reference*, Vol. 9 (eds Matyjaszewski, K. & Moeller, M.) 157–182 (Elsiver B.V., Amsterdam, 2012).
6. Chen, G.-Q. in *Plastics from Bacteria: Natural Functions and Applications*, Vol. 14 (ed Chen, G.-Q.) 17–37 (Springer-Verlag, Berlin, 2010).
7. Chen, G.-Q. A microbial polyhydroxyalkanoates (PHA) based bio- and materials industry. *Chem. Soc. Rev.* **38**, 2434–2446 (2009).
8. Lenz, R. W. & Marchessault, R. H. Bacterial polyesters: biosynthesis, biodegradable plastics and biotechnology. *Biomacromolecules* **6**, 1–8 (2005).
9. Sudesh, K., Abe, H. & Doi, Y. Synthesis, structure and properties of polyhydroxyalkanoates: biological polyesters. *Prog. Polym. Sci.* **25**, 1503–1555 (2000).
10. Poirier, Y., Nawrath, C. & Somerville, C. Production of polyhydroxyalkanoates, a family of biodegradable plastics and elastomers, in bacteria and plants. *Nat. Biotechnol.* **13**, 142–150 (1995).
11. Müller, H.-M. & Seebach, D. Poly(hydroxyalkanoates): a fifth class of physiologically important organic biopolymers? *Angew. Chem. Int. Ed. Engl.* **32**, 477–502 (1993).
12. Doi, Y. *Microbial Polyesters* (Wiley-VCH, New York, NY, 1990).
13. Tong, R. New chemistry in functional aliphatic polyesters. *Ind. Eng. Chem. Res.* **56**, 4207–4219 (2017).
14. Hillmyer, M. A. & Tolman, W. B. Aliphatic polyester block polymers: renewable, degradable, and sustainable. *Acc. Chem. Res.* **47**, 2390–2396 (2014).
15. Coulembier, O., Degée, P., Hedrick, J. L. & Dubois, P. From controlled ring-opening polymerization to biodegradable aliphatic polyester: especially poly (β-malic acid) derivatives. *Prog. Polym. Sci.* **31**, 723–747 (2006).
16. Mecking, S. Nature or petrochemistry?—biologically degradable materials. *Angew. Chem. Int. Ed.* **43**, 1078–1085 (2004).
17. Gross, R. A. & Kalra, B. Biodegradable polymers for the environment. *Science* **297**, 803–807 (2002).
18. Albertsson, A.-C. & Varma, I. K. Aliphatic polyesters: synthesis, properties and applications. *Adv. Polym. Sci.* **157**, 1–40 (2002).
19. Middleton, J. & Tipton, A. Synthetic biodegradable polymers as orthopedic devices. *Biomaterials* **21**, 2335–2346 (2000).
20. Mecerreyes, D., Jérôme, R. & Dubois, P. Novel macromolecular architectures based on aliphatic polyesters: relevance of the "coordination-insertion" ring-opening polymerization. *Adv. Polym. Sci.* **147**, 1–59 (1999).
21. Carpentier, J.-F. Rare-earth complexes supported by tripodal tetradentate bis (phenolate) ligands: a privileged class of catalysts for ring-opening polymerization of cyclic esters. *Organometallics* **34**, 4175–4189 (2015).
22. Jérôme, C. & Lecomte, P. Recent developments in ring-opening polymerization of lactones. *Adv. Polym. Sci.* **245**, 173–217 (2012).

23. Carpentier, J.-F. Discrete metal catalysts for stereoselective ring-opening polymerization of chiral racemic β-lactones. *Macromol. Rapid Commun.* **31**, 1696–1705 (2010).

24. Kiesewetter, M. K., Shin, E. J., Hedrick, J. L. & Waymouth, R. M. Organocatalysis: opportunities and challenges for polymer synthesis. *Macromolecules* **43**, 2093–2107 (2010).

25. Thomas, C. M. Stereocontrolled ring-opening polymerization of cyclic esters: synthesis of new polyester microstructures. *Chem. Soc. Rev.* **39**, 165–173 (2010).

26. Kamber, N. E. et al. Organocatalytic ring-opening polymerization. *Chem. Rev.* **107**, 5813–5840 (2007).

27. Dechy-Cabaret, O., Martin-Vaca, B. & Bourissou, D. Controlled ring-opening polymerization of lactide and glycolide. *Chem. Rev.* **104**, 6147–6176 (2004).

28. Okada, M. Chemical synthesis of biodegradable polymers. *Prog. Polym. Sci.* **27**, 87–133 (2002).

29. Jedlinski, Z., Kurcok, P. & Lenz, R. W. First facile synthesis of biomimetric poly-(R)-3-hydroxybutyrate via regioselective anionic polymerization of (S)-β-butyrolactone. *Macromolecules* **31**, 6718–6720 (1998).

30. Iida, M., Araki, T., Teranishi, K. & Tani, H. Effect of substituents on stereospecific polymerization of β-alkyl- and β-chloroalkyl-β-propiolactones. *Macromolecules* **10**, 275–284 (1977).

31. Teranishi, K., Iida, M., Araki, T., Yamashita, S. & Tani, H. Stereospecific polymerization of β-alkyl-β-propiolactone. *Macromolecules* **7**, 421–427 (1974).

32. Agostini, D. E., Undo, J. B. & Shelton, J. R. Synthesis and characterization of poly-β-hydroxybutyrate. I. Synthesis of crystalline DL-poly-β-hydroxybutyrate from DL-β-butyrolactone. *J. Polym. Sci. Part A1* **9**, 2775–2787 (1971).

33. Inoue, S., Tomoi, S., Tsuruta, T. & Furukawa, J. Organometallic-catalyzed polymerization of propiolactone. *Makromol. Chem.* **48**, 229–233 (1961).

34. Moore, T., Adhikari, R. & Gunatillake, P. Chemosynthesis of bioresorbable poly(γ-butyrolactone) by ring-opening polymerisation: a review. *Biomaterials* **26**, 3771–3782 (2005).

35. Martin, D. P. & Williams, S. F. Medical applications of poly-4-hydroxybutyrate: a strong flexible absorbable biomaterial. *Biochem. Eng. J.* **16**, 97–105 (2003).

36. Hong, M. & Chen, E. Y.-X. Completely recyclable biopolymers with linear and cyclic topologies *via* ring-opening polymerization of γ-butyrolactone. *Nat. Chem.* **8**, 42–49 (2016).

37. Wu, B. & Lenz, R. W. Stereoregular polymerization of [R,S]-3-butyrolactone catalyzed by alumoxane–monomer adducts. *Macromolecules* **31**, 3473–3477 (1998).

38. Jaimes, C. et al. Structure and morphology of poly([R,S]-β-butyrolactone) synthesized from aluminoxane catalyst. *Eur. Polym. J.* **34**, 175–185 (1998).

39. Bloembergen, S., Holden, D. A., Bluhm, T. L., Hamer, G. K. & Marchessault, R. H. Stereoregularity in synthetic β-hydroxybutyrate and β-hydroxyvalerate homopolyesters. *Macromolecules* **22**, 1656–1663 (1989).

40. Borgne, A. L. & Spassky, N. Stereoselective polymerization of β-butyrolactone. *Polymer (Guildf.)* **30**, 2312–2319 (1989).

41. Takeichi, T., Hieda, Y. & Takayama, Y. Asymmetric selective polymerization of β-butyrolactone catalyzed by optically active cobalt complex/triethylaluminum system. *Polym. J.* **20**, 159–162 (1998).

42. Rieth, L. R., Moore, D. R., Lobkovsky, E. B. & Coates, G. W. Single-site β-diiminate zinc catalysts for the ring-opening polymerization of β-butyrolactone and β-valerolactone to poly(3-hydroxyalkanoates). *J. Am. Chem. Soc.* **124**, 15239–15248 (2002).

43. Zintl, M. et al. Variably isotactic poly(hydroxybutyrate) from racemic β-butyrolactone: microstructure control by achiral chromium(III) salophen complexes. *Angew. Chem. Int. Ed.* **47**, 3458–3460 (2008).

44. Ajellal, N. et al. Polymerization of racemic β-butyrolactone using supported catalysts: a simple access to isotactic polymers. *Chem. Commun.* **46**, 1032–1034 (2010).

45. Kricheldorf, H. R. & Eggerstedt, S. Polylactones. 41. Polymerization of β-D,L-butyrolactone with dialkyltinoxides as initiators. *Macromolecules* **30**, 5693–5697 (1997).

46. Kemnitzer, J. E., McCarthy, S. P. & Gross, R. A. Syndiospecific ring-opening polymerization of β-butyrolactone to form predominantly syndiotactic poly (β-hydroxybutyrate) using tin(IV) catalysts. *Macromolecules* **26**, 6143–6150 (1993).

47. Bouyahyi, M., Ajellal, N., Kirillov, E., Thomas, C. M. & Carpentier, J.-F. Exploring electronic versus steric effects in stereoselective ring-opening polymerization of lactide and β-butyrolactone with amino-alkoxybis (phenolate)–yttrium complexes. *Chem. – Eur. J.* **17**, 1872–1883 (2011).

48. Ajellal, N. et al. Syndiotactic-enriched poly(3-hydroxybutyrate)s via stereoselective ring-opening polymerization of racemic β-butyrolactone with discrete yttrium catalysts. *Macromolecules* **42**, 987–993 (2009).

49. Amgoune, A., Thomas, C. M., Ilinca, S., Roisnel, T. & Carpentier, J.-F. Highly active, productive, and syndiospecific yttrium initiators for the polymerization of racemic β-butyrolactone. *Angew. Chem. Int. Ed.* **45**, 2782–2784 (2006).

50. Amgoune, A., Thomas, C. M., Roisnel, T. & Carpentier, J.-F. Ring-opening polymerization of lactide with group 3 metal complexes supported by dianionic alkoxy-amino-bisphenolate ligands: combining high activity, productivity, and selectivity. *Chem. – Eur. J.* **12**, 169–179 (2006).

51. Ligny, R., Hänninen, M. M., Guillaume, S. M. & Carpentier, J.-F. Highly syndiotactic or isotactic polyhydroxyalkanoates by ligand-controlled yttrium-catalyzed stereoselective ring-opening polymerization of functional racemic β-butyrolactone. *Angew. Chem. Int. Ed.* **56**, 10388–10393 (2017).

52. Drumright, R. E., Gruber, P. R. & Henton, D. E. Polylactic acid technology. *Adv. Mater.* **12**, 1841–1846 (2000).

53. Manso, J. A., Perez-Prior, M. T., Del Pilar Garcia-Santos, M., Calle, E. & Casado, J. A kinetic approach to the alkylating potential of carcinogenic lactones. *Chem. Res. Toxicol.* **18**, 1161–1166 (2005).

54. Arcana, M., Giani-Beaune, O., Schue, F., Amass, W., & Amass, A. Structure and morphology of poly(β-hydroxybutyrate) synthesized by ring-opening polymerization of racemic (R,S)-β-butyrolactone with distannoxane derivatives. *Polym. Int.* **49**, 1348–1355 (2000).

55. Tanahashi, N. & Doi, Y. Thermal properties and stereoregularity of poly(3-hydroxybutyrate) from optically active β-butyrolactone with a zinc-based catalyst. *Macromolecules* **24**, 5732–5733 (1991).

56. Zhang, Y., Gross, R. A. & Lenz, R. W. Stereochemistry of the ring-opening polymerization of (S)-β-butyrolactone. *Macromolecules* **23**, 3206–3212 (1990).

57. Seebach, D., Hoffmann, T., Kühnle, F. N. M., Kinkel, J. N. & Schulte, M. Preparation, structure, and properties of all possible cyclic dimers (diolides) of 3-hydroxybutanoic acid. *Helv. Chim. Acta* **78**, 1525–1540 (1995).

58. Seebach, D., Hoffmann, T., Kühnle, F. N. M., Kinkel, J. N. & Schulte, M. The triolide of (R)-3-hydroxybutyric acid—direct preparation from polyhydroxybutyrate and formation of a crown estercarbonyl complex with Na Ions. *Angew. Chem. Int. Ed.* **31**, 434–435 (1992).

59. Melchiors, M., Keul, H. & Höcker, H. Depolymerization of poly[(R)-3-hydroxybutyrate] to cyclic oligomers and polymerization of the cyclic trimer: an example of thermodynamic recycling. *Macromolecules* **29**, 6442–6451 (1996).

60. Melchiors, M., Keul, H. & Höcker, H. Synthesis of highly isotactic poly[(R)-3-hydroxybutyrate] by ring-opening polymerization of (R,R,R)-4,8,12-trimethyl-l,5,9-trioxacyclododeca-2,6,10-trione. *Macromol. Chem. Rapid Commun.* **15**, 497–506 (1994).

61. Hong, M., Tang, X., Newell, B. S. & Chen, E. Y.-X. 'Non-strained' γ-butyrolactone-based copolyesters: copolymerization characteristics and composition-dependent (thermal, eutectic, cocrystallization and degradation) properties. *Macromolecules* **50**, 8469–8479 (2017).

62. Tang, X. et al. The quest for converting biorenewable bifunctional α-methylene-γ-butyrolactone into degradable and recyclable polyester: controlling vinyl-addition/ring-opening/cross-linking pathways. *J. Am. Chem. Soc.* **138**, 14326–14337 (2016).

63. Liu, Q. et al. Cationic rare-earth metal SALEN complexes. *Dalton Trans.* **44**, 6170–6178 (2008).

64. Lin, M.-H. & RajanBabu, T. V. Ligand-assisted rate acceleration in transacylation by a yttrium-salen complex. Demonstration of a conceptually new strategy for metal-catalyzed kinetic resolution of alcohols. *Org. Lett.* **4**, 1607–1610 (2002).

65. DiCiccio, A. M., Longo, J. M., Rodríguez-Calero, G. G. & Coates, G. W. Development of highly active and regioselective catalysts for the copolymerization of epoxides with cyclic anhydrides: an unanticipated effect of electronic variation. *J. Am. Chem. Soc.* **138**, 7107–7113 (2016).

66. Char, J. et al. Microstructurally controlled polymers of *rac*-lactide by lithium complexes. *C. R. Chim.* **19**, 167–172 (2016).

67. Chen, H.-L., Dutta, S., Huang, P.-Y. & Lin, C.-C. Preparation and characterization of aluminum alkoxides coordinated on salen-type ligands: highly stereoselective ring-opening polymerization of *rac*-lactide. *Organometallics* **31**, 2016–2025 (2012).

68. Kochnev, A. I., Oleynik, I. I., Oleynik, I. V., Ivanchev, S. S. & Tolstikov, G. A. Synthesis of salicylaldehydes bearing bulky substituents in the positions 3 and 5. *Russ. Chem. Bull. Int. Ed.* **56**, 1125–1129 (2007).

69. Sanz, M. et al. Monocyclopentadienyl bis(phenoxo-imino)zirconium complexes as precatalyst for olefin polymerization. Stereospecific methylation of an imino group with formation of a zirconium–amido bond. *Organometallics* **23**, 5324–5331 (2004).

70. Larrow, J. F. et al. A practical method for the large-scale preparation of [N,N'-Bis(3,5-di-tert-butyl salicylidene)-1,2-cyclohexanediaminato2(-)]manganese (III) chloride, a highly enantioselective epoxidation catalyst. *J. Org. Chem.* **59**, 1939–1942 (1994).

71. Casiraghi, G., Casnati, G., Puglia, G., Sartori, G. & Terenghi, G. Selective reactions between phenols and formaldehyde. A novel route to salicylaldehydes. *J. Chem. Soc. Perkin Trans. 1* **0**, 1862–1865 (1980).

72. Barham, P. J., Keller, A., Otun, E. L. & Holmes, P. A. Crystallization and morphology of a bacterial thermoplastic: poly-3-hydroxybutyrate. *J. Mater. Sci.* **19**, 2781–2794 (1984).

Author contributions

X.T. and E.Y.-X.C. conceived the idea and designed the experiments. X.T. performed the experiments. X.T. and E.Y.-X.C. co-wrote the manuscript and participated in data analyses and discussions. E.Y.-X.C. directed the project.

Additional information

Supplementary Information accompanies this paper at https://doi.org/10.1038/s41467-018-04734-3.

Competing interests: E.Y.-X. C. and X.T. are inventors on U.S. patent applications 62/616277 and 62/671,069, submitted by Colorado State University Research Foundation, which covers the herein described chemical synthesis of P3HB and kinetic resolution of *rac*-DL.

Reprints and permission information is available online at http://npg.nature.com/reprintsandpermissions/

Publisher's note: Springer Nature remains neutral with regard to jurisdictional claims in published maps and institutional affiliations.